ChemistrySELECT

Supporting Information

Polymer Brush-Modified Microring Resonators for Partition-Enhanced Small Molecule Chemical Detection

Alexandria L. D. Stanton, Kali A. Serrano, Professor Paul V. Braun,* and Professor Ryan C. Bailey*

Table of Contents

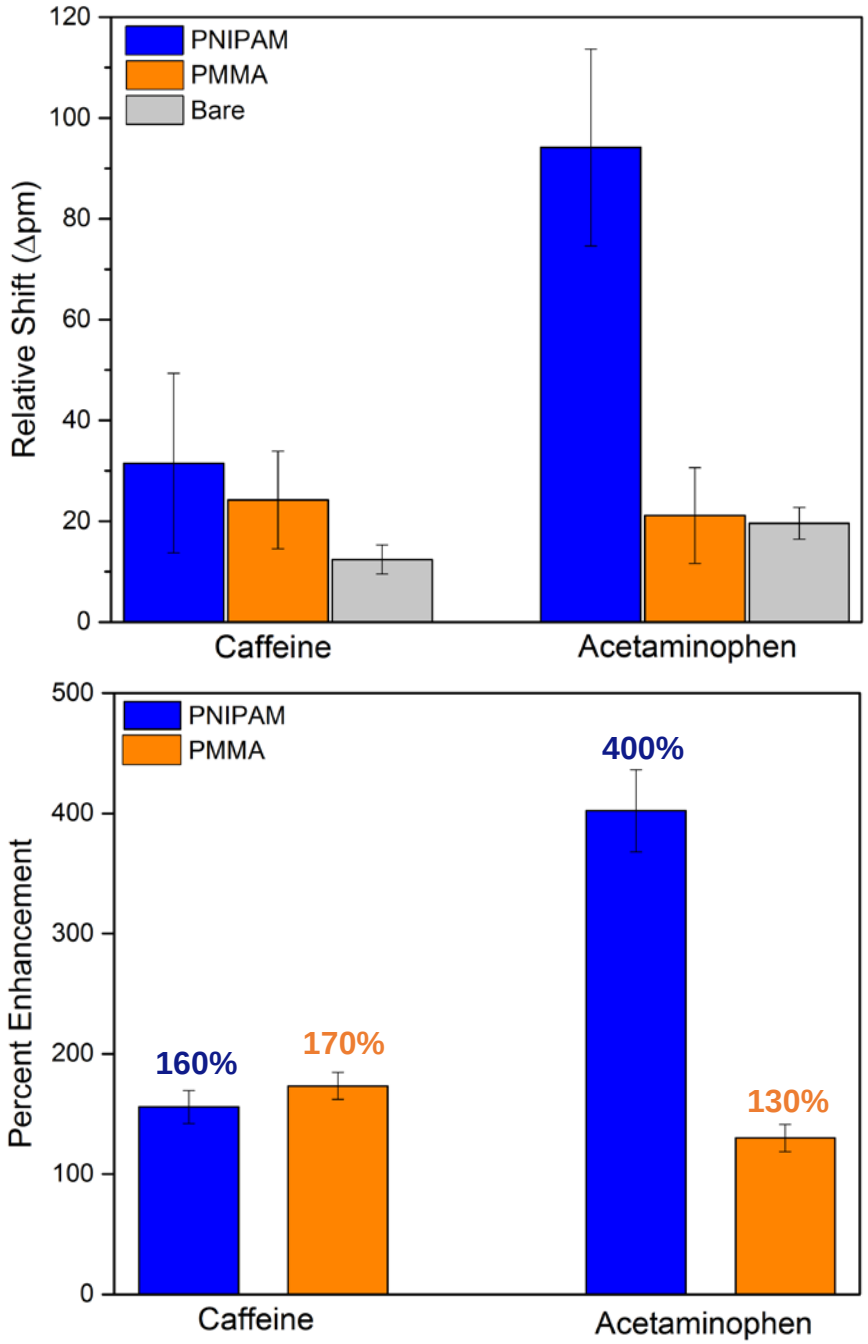

Figure S1: Non-corrected (not subtracted) and percent enhancement for acetaminophen and caffeine detection (corresponding to Figure 2)

A) Non-corrected resonance wavelength shifts for caffeine and acetaminophen detection, including bare- and two sets of polymer brush-modified microring sensors exposed to 10 mM aqueous solutions of both analytes. **B)** Percent detection enhancement values noted on plot were determined by dividing polymer brush-modified responses by bare microring sensor response.

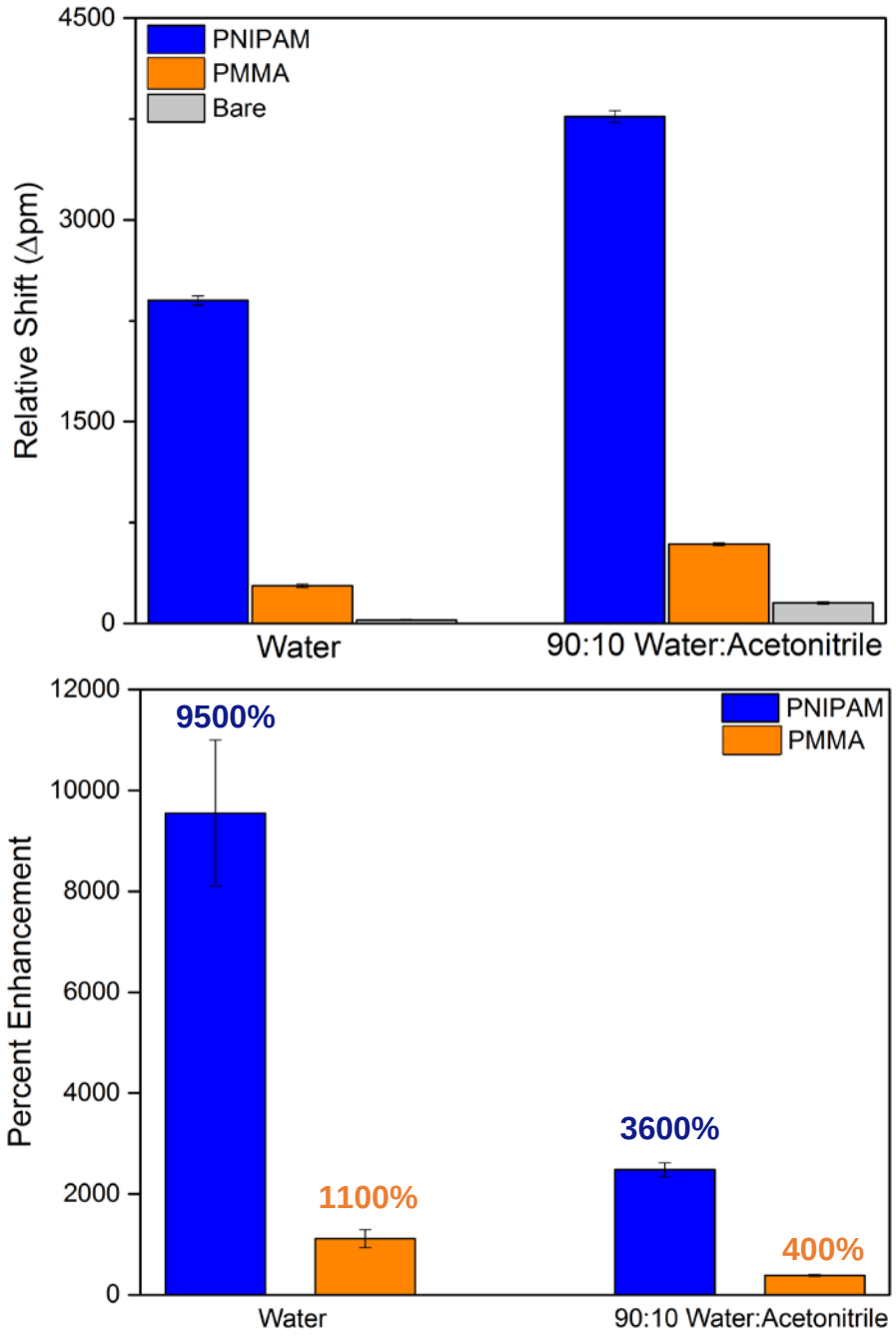

Figure S2: Non-corrected (not subtracted) and percent enhancement for Bisphenol A detection in water and 90:10 water:acetonitrile (corresponding to Figure 3)
A) Non-corrected resonance wavelength shifts for glyphosate detection, including bare- and two sets of polymer brush-modified microring sensors exposed to 10 mM solutions of Bisphenol A. **B)** Percent detection enhancement values noted on plot were determined by dividing polymer brush-modified responses by bare microring sensor response.

Alcohol partitioning into PMMA and PDMAEMA: Description, results, and discussion

To further investigate the interactions of solution-phase analytes with different polymer brush chemistries, we studied the partitioning of aqueous solutions of methanol, ethanol, and octanol with microring sensors presenting hydrophobic PMMA and hydrophilic PDMAEMA polymer brushes. These polymer brushes had dry thicknesses of 65 and 40 nm, respectively, as determined on blank silicon wafers grown in the same ATRP reaction flask via spectroscopic ellipsometry. This set of experiments focused on a single class of small molecule targets—alcohols—and was designed to examine the role of hydrophobicity and polymer solubility in a systematic way. The real-time resonance shifts accompanying exposure to these solutions, as well as the resonance shifts measured with a blank microring sensor (no polymer brush) are shown in Figure S3.

For methanol and ethanol, both of which are highly water-miscible, the hydrophilic PDMAEMA showed large negative resonance shifts, whereas hydrophobic PMMA showed a response similar to the blank microring, indicating no analyte partitioning. For octanol, which is significantly more hydrophobic (much less miscible with water), highly differential responses were observed, with PMMA-modified sensors showing a positive shift in resonance wavelength larger than the blank ring, while PDMAEMA brushes showed a negative shift. The opposite signs of these shifts suggest that the resonance shifts are reflective of partitioning according to intermolecular forces. In this case, this is a combination of solubility and hydrophobicity differences between the analytes and two different polymer brush chemistries.

Compound	δ [(MPa)$^{0.5}$]
Water	48.0[1]
Methanol	29.7[2]
Ethanol	26.1[2]
Octanol	21.0[1]
PMMA	20.0[2]
PDMAEMA	unknown

To help explain these responses it is important to consider the solubility parameters, δ, of the compounds involved in this interaction, which are listed in table at right. Equivalent solubility parameters suggest that compounds are miscible, or are a good solvent combination. First considering the responses of PMMA, we found that there was no difference in response from PMMA-modified microrings compared with bare microring sensors, and this is consistent with the fact that methanol and ethanol do not interact with PMMA. However, when exposed to octanol, which has a solubility parameter similar to PMMA, we see a positive resonance wavelength shift, consistent with the notion that octanol can partition into the polymer brush.

The interactions of the alcohols with PDMAEMA is somewhat more complex, and the solubility parameter for this polymer is unknown. However, the hydrophilic nature of PDMAEMA and literature reports suggest that both methanol[3] and ethanol[4] are good solvents for this

polymer. By contrast, one would not expect octanol to be as good of a solvent considering it more hydrophobic nature. PDMAEMA is also soluble in water and upon flowing water across these initially dry polymer brushes, brush hydration is observed as a positive shift in resonance wavelength. The addition of both ethanol and methanol leads to a large negative shift in the resonance wavelength. The magnitude of the shift is understandable on account of the high solubility of these alcohols in the polymer brush.

The negative direction of the shift for PDMAEMA exposed to ethanol and octanol is explained by the fact that the polymer brush is likely swelling as to extend beyond the evanescent field of the sensor, replacing higher refractive index polymer ($n \approx 1.42$) with much lower index water ($n = 1.33$) and methanol ($n = 1.329$) or ethanol ($n = 1.36$). The original PDMAEMA brush was 40 nm thick when fully dried, and is expected to be ~60 nm when hydrated. This is already nearly equivalent to the 1/e decay length of the microrings evanescent field sensitivity profile. While the resonators are still sensitive to refractive index at and beyond this distance from the surface, the relative sensitivity to changes in this region are less than the same RI changes nearer the surface. Moreover, it was previously determined that "ethanol is a more effective solvent for PDMAEMA than water."[4] Therefore additional partitioning of ethanol into the polymer brush would likely lead to additional polymer swelling. Moreover, as mentioned above, as the polymer brush swells beyond into this less sensitive distance from the surface, the extended PDMAEMA is replaced by lower refractive index water and alcohol, effectively lowering the n_{eff} sampled by the optical mode and leading to a negative resonance wavelength shift. When exposed to octanol, negative resonance shifts are again observed for PDMAEMA; however, their magnitude is reduced because octanol is a poorer solvent for this polymer.

It is worthwhile to point out that the responses from PDMAEMA upon cycling from water to methanol and ethanol appear somewhat irregular, but the negative shift in the alcohol solution followed by positive shift in water is consistent. The irregularity of the "shape" of the response is something that will require additional studies to fully understand; however, it is perhaps not surprising given the complexities of these solubility/hydration interactions. Also, it is important to note the difference between simple swelling and brush strand dissolution. Many compounds will penetrate a chemical film, simply diffusing in at a rate dictated by penetrant size and brush matrix, but the localized relaxation of the brush in the presence of a penetrant is classified as dissolution. Dissolution of the brush structure is likely concentration-dependent and defined by non-Fickian transport. Our measurement is likely sensitive to brush extension and dissolution as that changes the relative occupancy of the evanescent field by higher RI polymer and lower RI water/alcohols, and the partition kinetics are complex and warrant future studies.

By comparison, PMMA, which only shows partitioning of octanol, is a glassy polymer., in contrast to PDMAEMA. Dissolution is be more likely to occur in a “Case II” manner where a sharp front distinguishes swollen and unswollen regions, while a front of solvent penetrates at a constant rate.[5] This more well-defined and more limited partitioning may explain the more well-behaved shifts in resonance wavelength. Also, the refractive index of octanol (n = 1.429) is closer to that of the polymer brush so that any volume replaced by this solvent might still support a positive resonance shift.

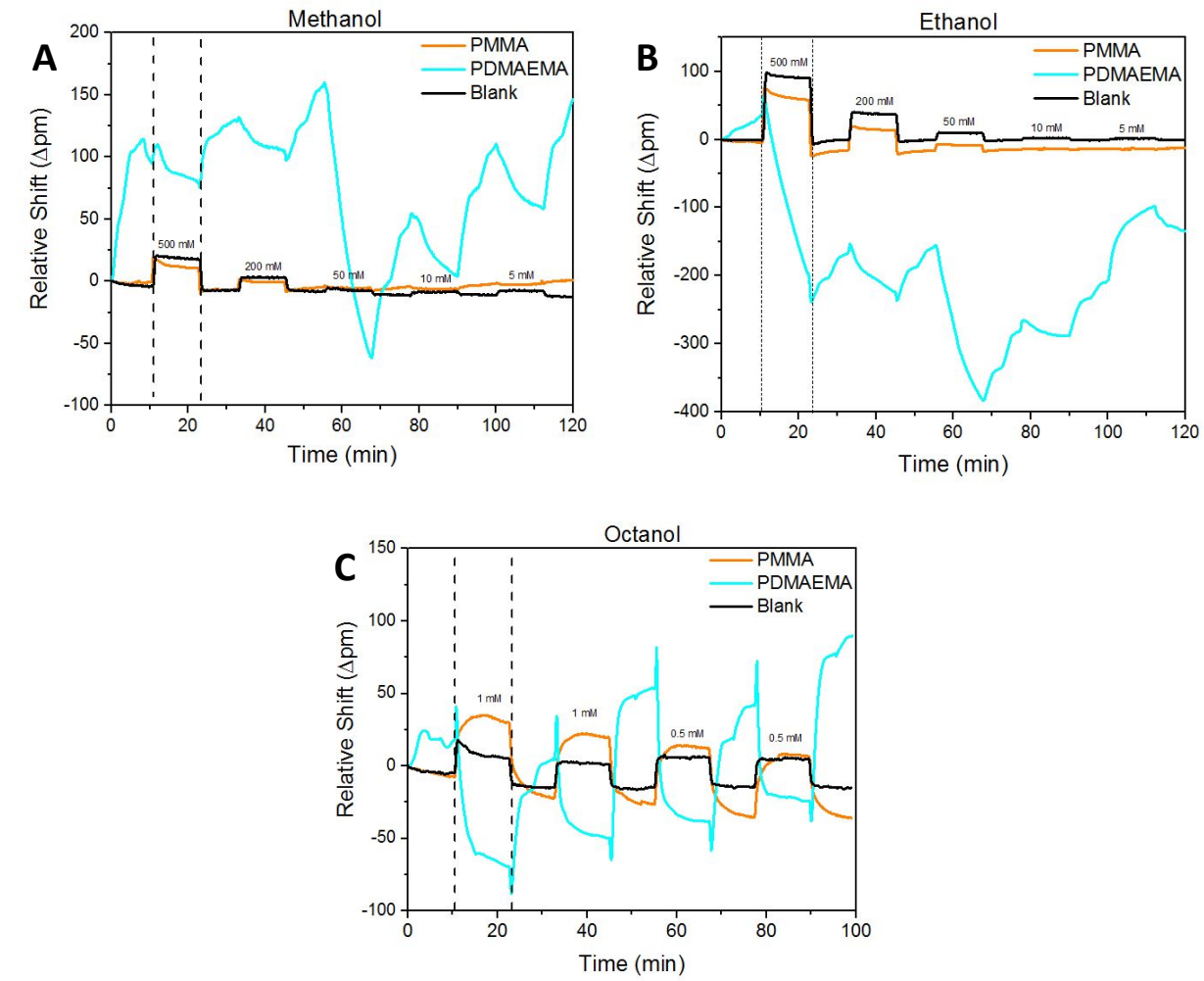

Figure S3: Real-time resonance shifts of PMMA and PDMAEMA-modified microring resonators to aqueous solutions of methanol, ethanol, and octanol.

Response of polymer brush-modified and bare microring resonators to aqueous solutions of methanol, ethanol, and octanol in decreasing concentrations at noted. Pure water and alcohol-containing aqueous solutions are cycled at 10 minute intervals. The magnitudes and directions of responses are explained in the above discussion. **A)** Exposure to methanolic solutions show large magnitude shifts for PDMAEMA-modified rings due to strong solubility of methanol in the polymer brush. The response of PMMA-modified rings is equivalent to bare microring indicating no partitioning. **B)** Exposure to ethanolic solutions shows similar behavior; strong interactions with PDMAEMA and nothing for PMMA. **C)** Exposure to octanolic solutions elicits responses from both PMMA and PDMAEMA-modified microrings on account of octanol being an interacting solvent for both polymer brushes. Both responses are distinctly different from that of bare microrings.

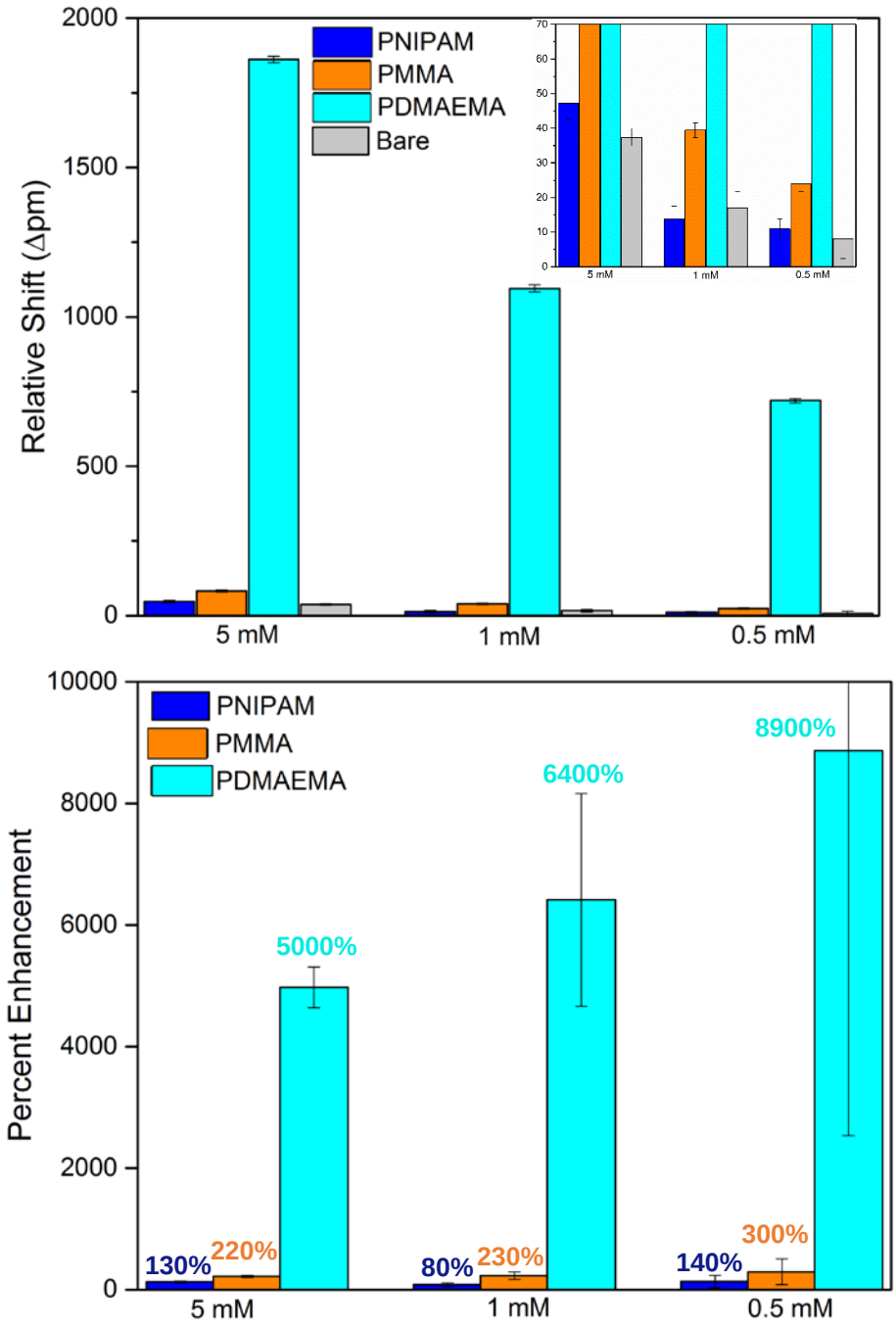

Figure S4: Non-corrected (not subtracted) and percent enhancement for 4-methylumbelliferyl phosphate detection (corresponding to Figure 4a)
A) Non-corrected resonance wavelength shifts for 4-methylumbelliferyl phosphate detection, including bare- and three sets of polymer brush-modified microring sensors at four different concentrations of 4-methylumbelliferyl phosphate. **B)** Percent detection enhancement values noted on plot were determined by dividing polymer brush-modified responses by bare microring sensor response.

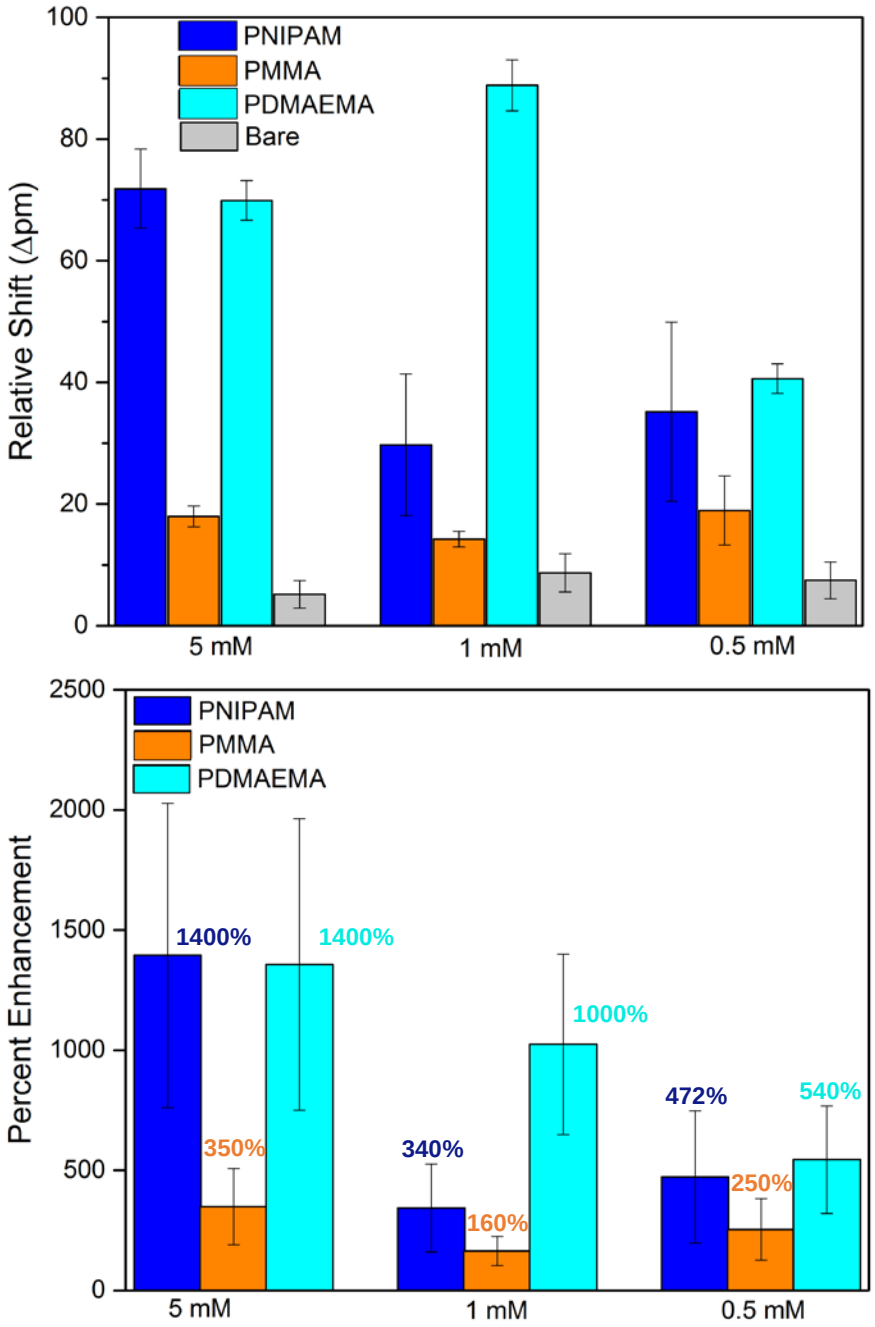

Figure S5: Non-corrected (not subtracted) and percent enhancement for glyphosate detection (corresponding to Figure 4b)
A) Non-corrected resonance wavelength shifts for glyphosate detection, including bare- three sets of polymer brush-modified microring sensors at four different glyphosate concentrations.
B) Percent detection enhancement values noted on plot were determined by dividing polymer brush-modified responses by bare microring sensor response.

Detailed description of microring resonator sensing technology

Silicon photonic microring resonators, which belong to a larger class of whispering gallery resonators,[6] are chip-integrated optical structures that are responsive to changes in the local refractive index near the sensor surface. In these devices, shown schematically in Figure S5, light from an adjacent linear waveguide can be coupled into the microring cavity only under conditions of optical resonance, as defined by: coupled into the cavity via an adjacent linear waveguide positioned within the evanescent field. Optical modes are supported along the circumference of the cavity according to the resonance condition:

$$m\lambda = 2\pi r n_{eff} \quad \text{(S1)}$$

where m is an integer, λ is wavelength of light, r is the radius of the resonator, and n_{eff} is the effective refractive index sampled by the optical mode. Light is confined into the resonator via total internal reflection and interacts with the environment through an exponentially-decaying optical profile that has a 1/e decay length of 63 nm.[7]

These devices are fabricated at the wafer scale on silicon-on-insulator wafers at a commercial silicon foundry using standard deep UV photolithography. High fidelity fabrication leads to high Q factor cavities which leads to a dramatic increase in the effective optical path length and dramatic sharpening of the resonance to an extremely narrow spectral dispersion (FWHM ≈ 50 picometers). As the refractive index near the resonator changes, in this case due to the localization of analytes via partitioning into the polymer brush, the local refractive index is changed, resulting in a shift in the resonance wavelengths of modes supported by the cavity. This provides the signal transduction mechanism.

This technology, which has been previously demonstrated for the detection of a range of biomolecular targets,[8–11] is being commercialized by Genalyte, Inc. as the Maverick detection platform. In the current configuration, each sensor array chip is 4 x 6 mm in size and features 132 individually-addressable, 30 µm-diameter sensors. The entire chip is coated with a fluoropolymer cladding layer and selectively removed to expose only 128 of the rings to solution. The remaining sensors can be used to correct for thermal drift. Each microring is optically addressed via input and output grating couplers, which are connected to either end of the linear coupling waveguide. In this way, all optical interfaces are done in the far field with light coupled from free-space into and off of the chip from the laser and then to a detection photodiode. No end coupling using fiber optics is required. Resonance measurements are made by sweeping the output of a tunable external cavity diode laser centered at 1.56 µm through a suitable spectral range and detecting resonances as dips in the optical power transmitted through the coupling waveguide past the microring sensor (Figure S5a—right).

During the detection experiment, the shift in resonance wavelength is determined in real-time with solutions being flowed across the sensor chip via an automated fluid handling system that delivers fluid through a laser cut Mylar gasket, which defined two channels per sensor array chip.

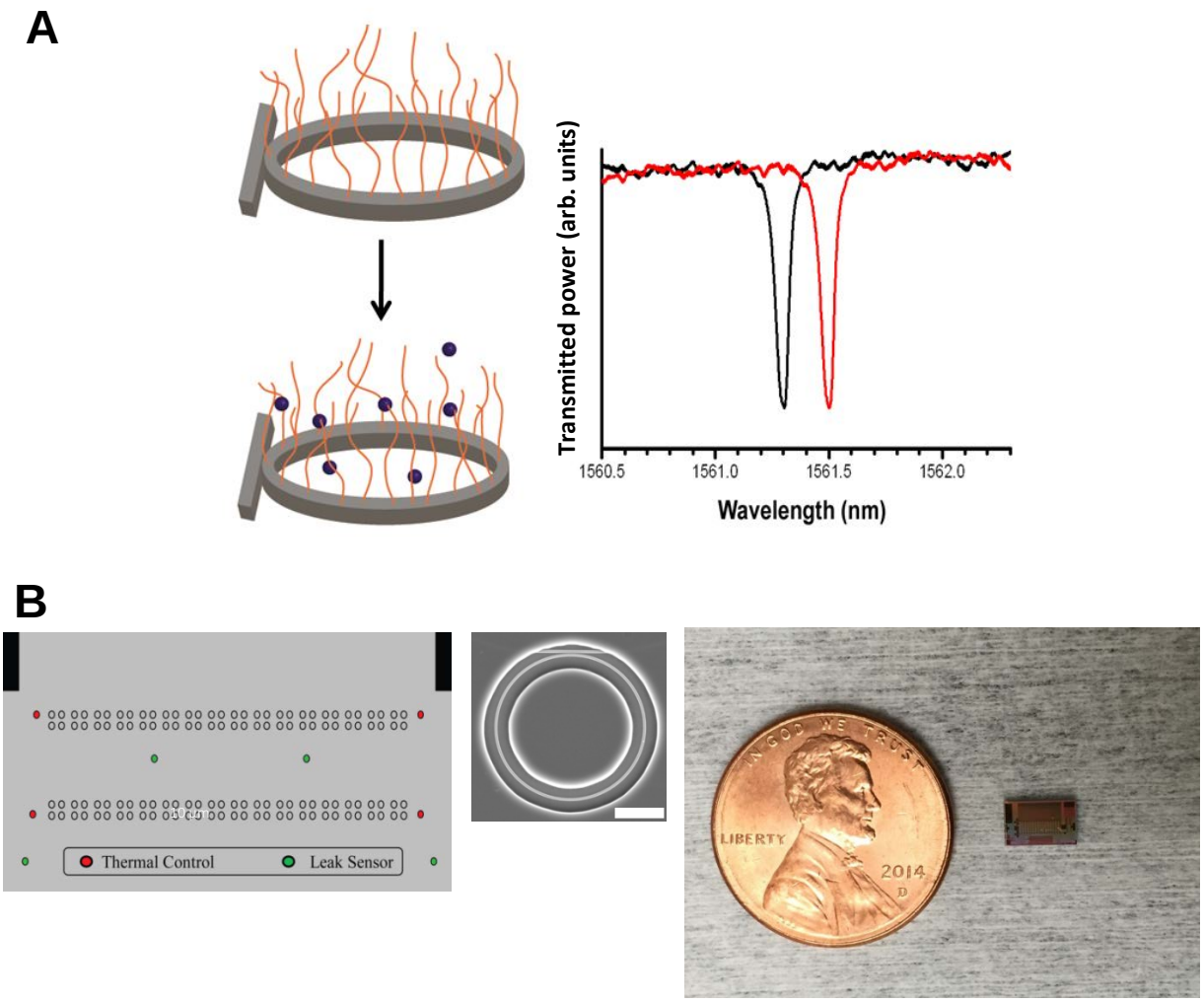

Figure S6: Silicon photonic microring resonator technology and sensor chip layout
A) Schematic diagram of polymer brush-modified microring resonator. Analyte localization within the polymer brush changes the local refractive index leading to a shift in resonance wavelength. A representative transmission spectra shows a decrease in optical power past the resonator at the resonance wavelength. A change in local refractive index accompanying analyte partitioning causes a shift in the resonance.**B)** Representative layout of a micoring resonator chip, with an SEM image of a single ring (scale bar 10 µm). An optical micrograph with a penny for scale reference.

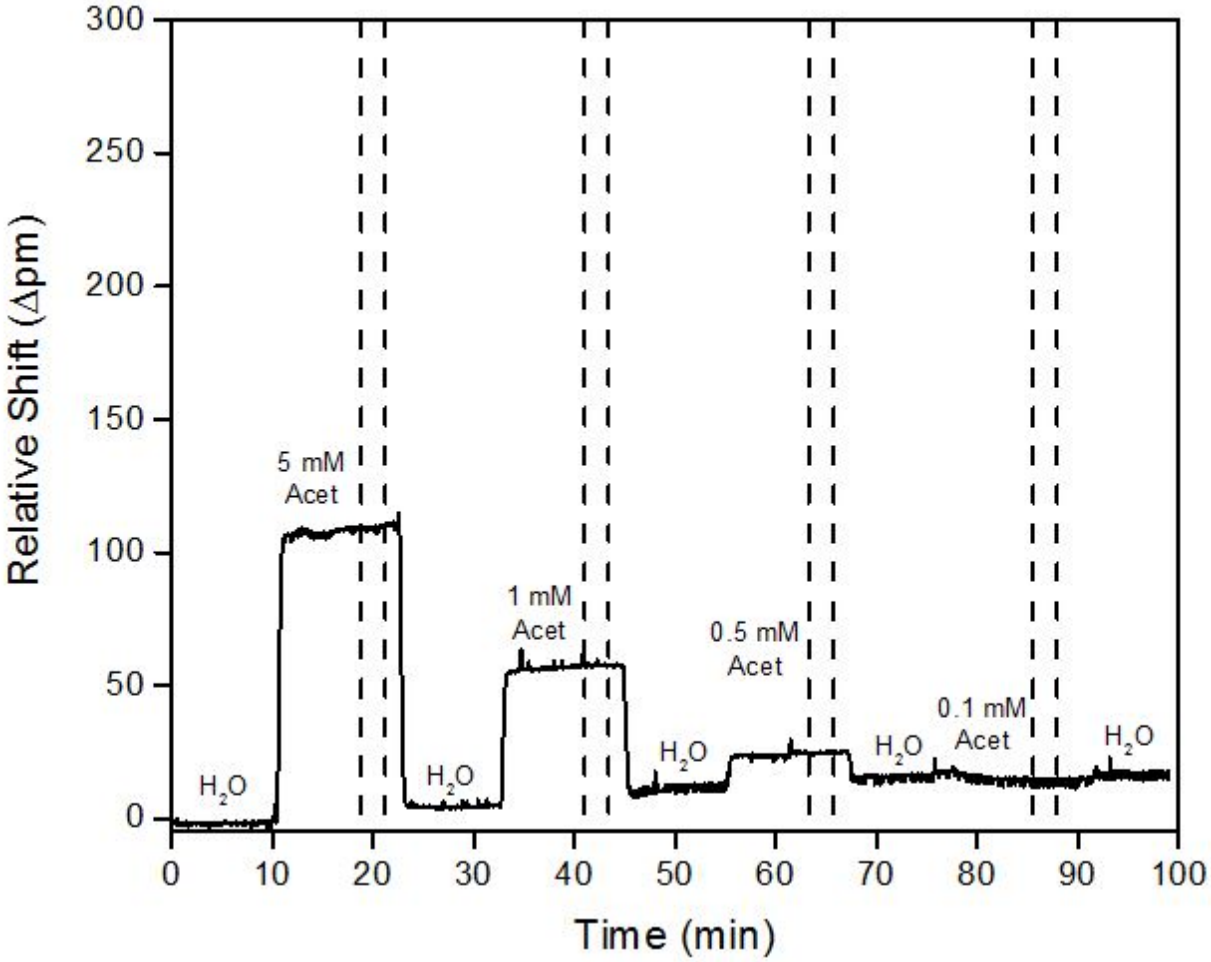

Figure S7: Example of a real-time resonance shift data during a detection experiment
The real-time response of a PNIPAM brush to a series of acetaminophen solutions (corresponding bar graph in Figure 2). The plateaued regions in between dotted vertical lines indicate where data was taken to generate bar graphs.

Experimental Section

Hydrophilic poly(N-Isopropylacrylamide) (PNIPAM),[12] hydrophilic poly(2-dimethylamino-ethylmethacrylate) (PDMAEMA),[13] and hydrophobic poly(methyl methacrylate) (PMMA)[14] polymer brushes were grown off the microring resonator substrates using adapted literature surface-initiated, atom-transfer radical polymerization (SI-ATRP) procedures. First, the silicon microring resonator chips were cleaned using oxygen plasma. Then, self-assembled monolayers of the initiator 11-(2-bromo-2-methyl)-propionyl undecyl tricholorosilane were formed on the substrates by immersion in a 1 mM hexane solution for 24 hours. After being rinsed in fresh hexane and dried under a nitrogen stream, the microchips were placed in a reaction vessel. 1,1,4,7,10,10-hexamethyltriethylene tetramine (HMTETA) was used for the ligand[15] and standard Schlenk techniques were used to transfer appropriate ratios of [monomer]:[Cu(I)]:[Cu(I)]:[ligand] into the reaction vessel. The polymeric substrates were rinsed with THF, IPA, and H_2O and then dried under a stream of nitrogen. Dry polymer thicknesses were measured using single wavelength ellipsometry (Gaertner L116C). The modified chips were exposed to the analytes via integrated microfluidics within the Genalyte Maverick M1 optical scanning instrumentation, whose operation has been described previously.[9] Text and a figure (Figure S6) describing the technology in greater detail can be found in the SI. Four microring resonators were monitored to determine both either bare- or polymer brush-modified sensor response, while four occluded rings were used for real-time temperature correction. The sensor responses are measured in real-time (see Figure S7 for a representative data trace) and extracted resonance wavelength shifts averaged over a suitable time period are plotted in Figures 2-4 for exposure to different small molecule analytes.

References

(1) Xu, H.; Song, J.; Tian, T.; Feng, R. Estimation of Organogel Formation and Influence of Solvent Viscosity and Molecular Size on Gel Properties and Aggregate Structures. *Soft Matter* **2012**, 0–12.

(2) Groele, R. J.; Krasicky, P. D.; Chun, S.-W.; Sullivan, J.; Rodriguez, F. Dissolution Rates of Poly (Methyl Methacrylate) in Mixtures of Nonsolvents. *J. Appl. Polym. Sci.* **1991**, *42*, 3–8.

(3) Mao, B. W.; Gan, L. H.; Gan, Y. Y. Ultra High Molar Mass poly[2-(Dimethylamino)ethyl Methacrylate] via Atom Transfer Radical Polymerization. *Polymer (Guildf).* **2006**, *47*, 3017–3020.

(4) Samal, S.; Dubruel, P. *Cationic Polymers in Regenerative Medicine*; RSC Polymer Chemistry Series; The Royal Society of Chemistry, 2015.

(5) Papanu, J. S.; Hess, D. W.; Soong, D. S. S.; Bell, A. T. Swelling of Poly (Methyl Methacrylate) Thin Films in Low Molecular Weight Alcohols. *J. Appl. Polym. Sci.* **1990**, *39*, 803–823.

(6) Wade, J. H.; Bailey, R. C. Applications of Optical Microcavity Resonators in Analytical Chemistry. *Annu. Rev. Anal. Chem.* **2016**, *9*, 1–25.

(7) Luchansky, M. S.; Washburn, A. L.; Martin, T. a.; Iqbal, M.; Gunn, L. C.; Bailey, R. C. Characterization of the Evanescent Field Profile and Bound Mass Sensitivity of a Label-Free Silicon Photonic Microring Resonator Biosensing Platform. *Biosens. Bioelectron.* **2010**, *26*, 1283–1291.

(8) Qavi, A. J.; Mysz, T. M.; Bailey, R. C. Isothermal Discrimination of Single-Nucleotide Polymorphisms via Real-Time Kinetic Desorption and Label-Free Detection of DNA Using Silicon Photonic Microring Resonator Arrays. *Anal. Chem.* **2011**, *83*, 6827–6833.

(9) Washburn, A. L.; Gunn, L. C.; Bailey, R. C. Label-Free Quantitation of a Cancer Biomarker in Complex Media Using Silicon Photonic Microring Resonators. *Anal. Chem.* **2009**, *81*, 9499–9506.

(10) Qavi, A. J.; Bailey, R. C. Multiplexed Detection and Label-Free Quantitation of MicroRNAs Using Arrays of Silicon Photonic Microring Resonators. *Angew. Chemie - Int. Ed.* **2010**, *49*, 4608–4611.

(11) McClellan, M. S.; Domier, L. L.; Bailey, R. C. Label-Free Virus Detection Using Arrays of Silicon Photonic Microring Resonators. *Biosens. Bioelectron.* **2012**, 388–392.

(12) Xue, C.; Yonet-Tanyeri, N.; Brouette, N.; Sferrazza, M.; Braun, P. V.; Leckband, D. E. Protein Adsorption on poly(N -Isopropylacrylamide) Brushes: Dependence on Grafting Density and Chain Collapse. *Langmuir* **2011**, *27*, 8810–8818.

(13) Koo, H. J.; Waynant, K. V.; Zhang, C.; Braun, P. V. Polymer Brushes Patterned with Micrometer-Scale Chemical Gradients Using Laminar Co-Flow. *ACS Appl. Mater. Interfaces* **2014**, *6*, 14320–14326.

(14) Ramakrishnan, a.; Dhamodharan, R.; Rühe, J. Controlled Growth of PMMA Brushes on Silicon Surfaces at Room Temperature. *Macromol. Rapid Commun.* **2002**, *23*, 612–616.

(15) Millard, P.-E.; Mougin, N. C.; Böker, A.; Müller, A. H. E. Fast ATRP of N-Isopropylacrylamide in Water and Its Application to Bioconjugates. *Polym. Prepr. (American Chem. Soc. Div. Polym. Chem.* **2008**, *49*, 121.